



## Supporting Information

for *Adv. Energy Mater.*, DOI: 10.1002/aenm.202103215

2D/3D Hybrid Cs<sub>2</sub>AgBiBr<sub>6</sub> Double Perovskite Solar Cells:  
Improved Energy Level Alignment for Higher Contact-  
Selectivity and Large Open Circuit Voltage

*Maximilian T. Sirtl, Rik Hooijer, Melina Armer, Firouzeh  
G. Ebadi, Mahdi Mohammadi, Clément Maheu, Andreas  
Weis, Bas T. van Gorkom, Sebastian Häringer, René  
A. J. Janssen, Thomas Mayer, Vladimir Dyakonov,  
Wolfgang Tress, and Thomas Bein\**

# Supporting Information

## **2D/3D Hybrid Cs<sub>2</sub>AgBiBr<sub>6</sub> Double Perovskite Solar Cells: Improved Energy Level Alignment for Higher Contact-Selectivity and Large Open Circuit Voltage**

Maximilian T. Sirtl, Rik Hooijer, Melina Armer, Firouzeh G. Ebadi, Mahdi Mohammadi, Clément Maheu, Andreas Weis, Bas T. van Gorkom, Sebastian Häringer, René A. J. Janssen, Thomas Mayer, Vladimir Dyakonov, Wolfgang Tress and Thomas Bein\*

M. T. Sirtl, R. Hooijer, A. Weis, S. Häringer, T. Bein: Department of Chemistry and Center for NanoScience (CeNS), University of Munich (LMU) Butenandtstr. 11, 81377 Munich, Germany

M. Armer, V. Dyakonov: Experimental Physics VI, Julius Maximilian University of Würzburg, 97074 Würzburg, Germany

F. Ebadi, M. Mohammadi, W. Tress: Institute of Computational Physics (ICP), ZHAW School of Engineering, Wildbachstr. 21, Winterthur 8400, Switzerland

C. Maheu, T. Mayer: Surface Science Laboratory, Department of Materials and Earth Sciences, Technical University of Darmstadt, Otto-Berndt-Strasse 3, 64287 Darmstadt, Germany

B.T. van Gorkom, R.A.J. Janssen: Molecular Materials and Nanosystems & Institute for Complex Molecular Systems, Eindhoven University of Technology, Eindhoven 5600 MB, Netherlands

e-mail: bein@lmu.de

**keywords:** Double Perovskite; Cs<sub>2</sub>AgBiBr<sub>6</sub>; 2D/3D hybrid perovskite; double perovskite solar cells; 2D perovskite

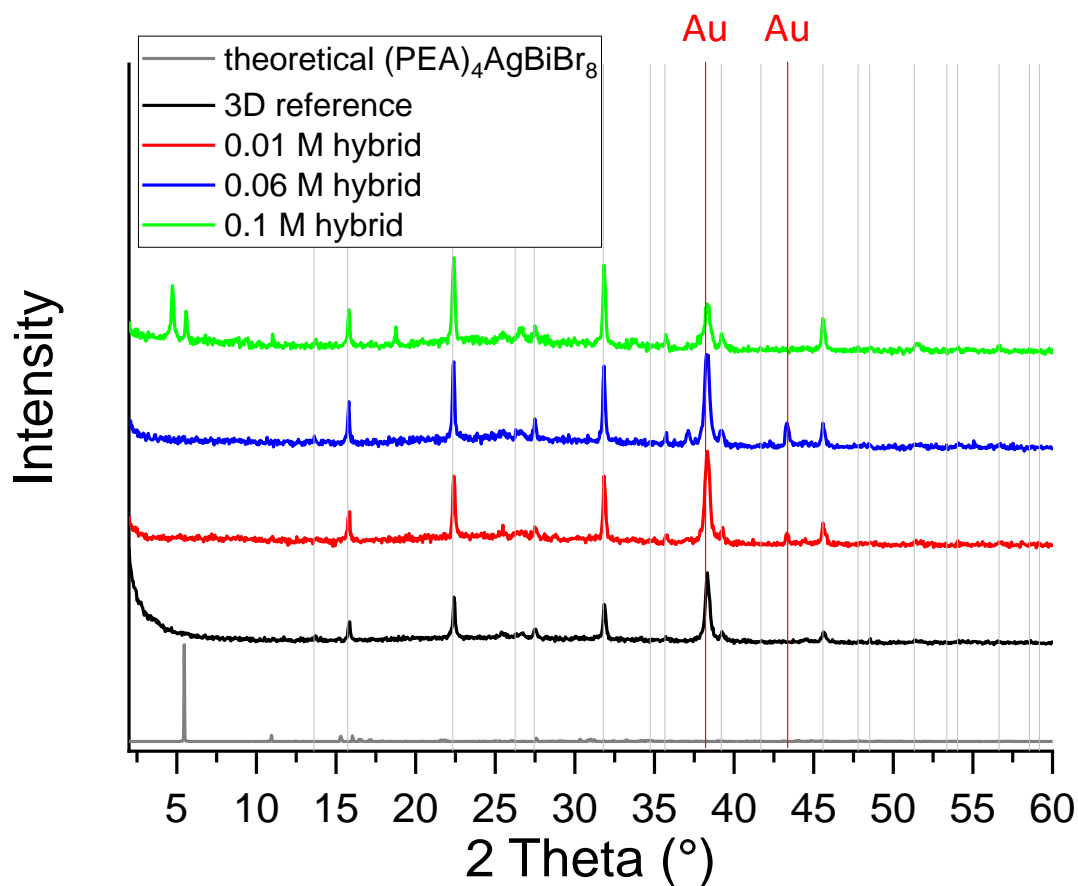


Figure S 1: Full XRD patterns of the different thin films recorded in Bragg Brentano Geometry. The grey line shows the theoretical pattern of (PEA)<sub>4</sub>AgBiBr<sub>8</sub> perovskite. The grey drop lines indicate the theoretical pattern of the 3D double perovskite Cs<sub>2</sub>AgBiBr<sub>6</sub>. The black line is the obtained pattern from the pure 3D solar cell, the red line shows the experimental pattern of the solar cell with the 0.01 M hybrid as active layer, the blue and green line show the experimental patterns of solar cells comprising the 0.06 M and 0.1 M hybrid respectively. The red drop line indicates the reflections arising from the gold electrode.

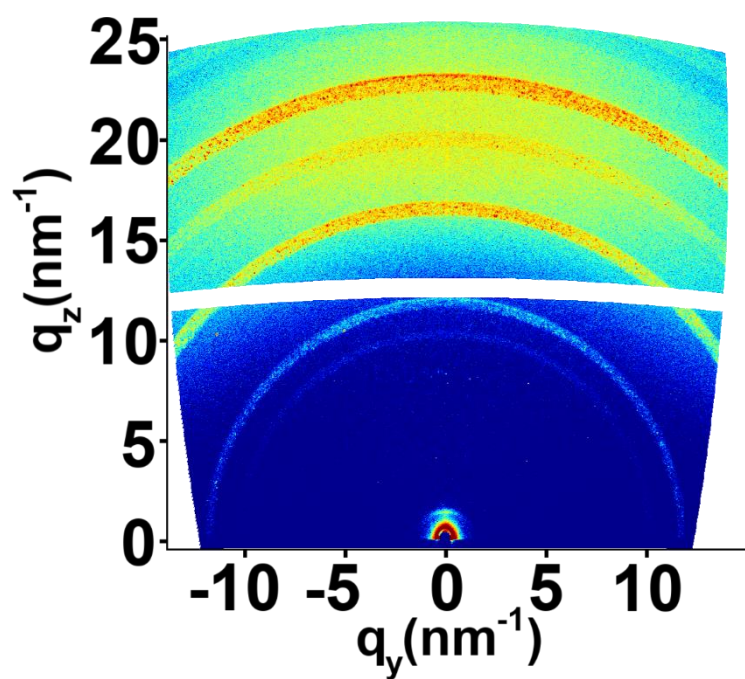


Figure S 2: Detector-image of GIWAXS measurement performed on thin films treated with 0.01 M PEABr and measured with an increased integration time.

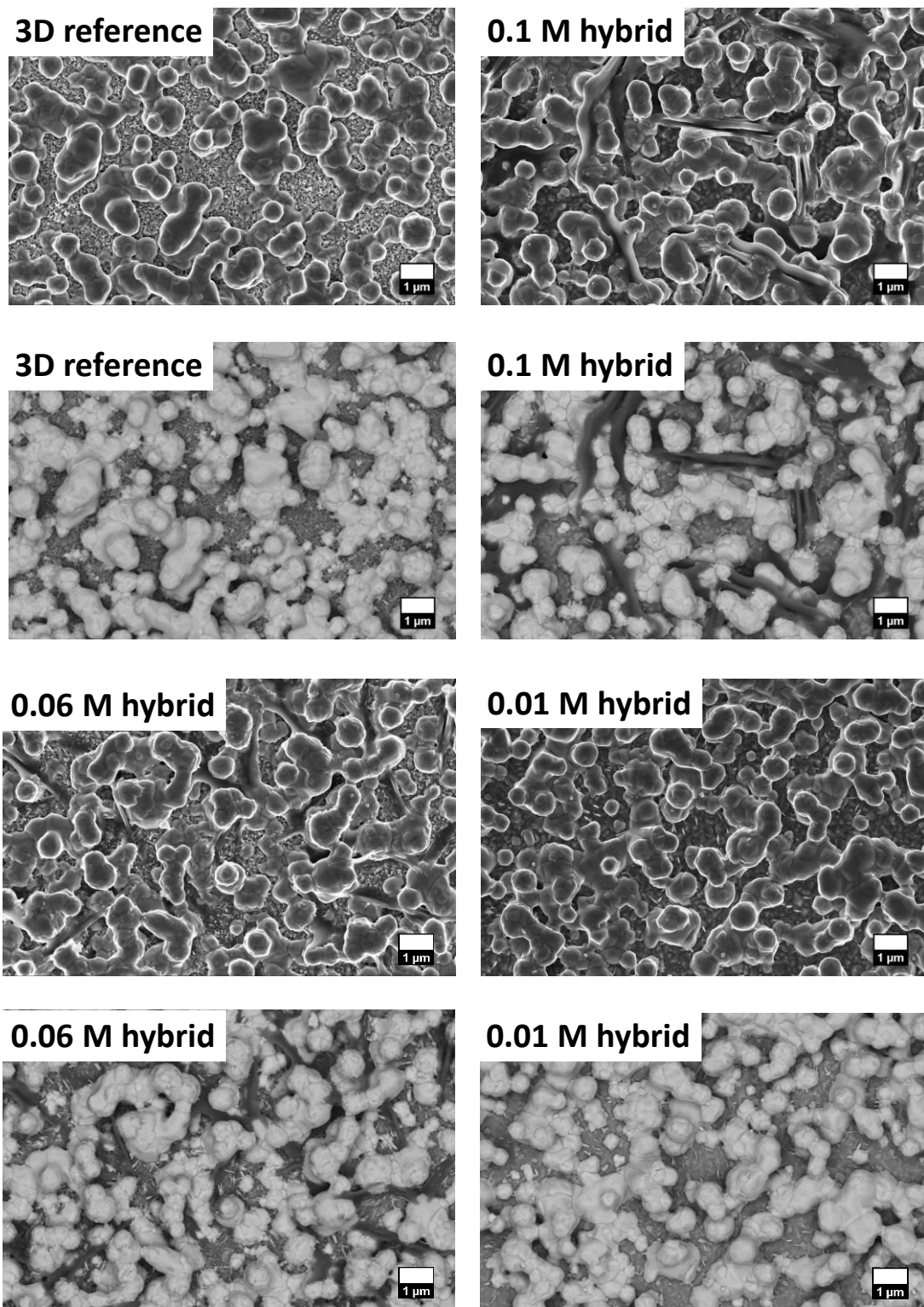


Figure S 3: SEM topview images of the investigated thin films. Top line shows the through-lens detector (TLD) images. Lower line shows the images obtained with a circular backscatter detector (CBS). The 3D reference is shown on the left upper side, the 0.1 M hybrid in the right upper and the 0.06 M hybrid on the left lower side and the 0.01 M on the right lower side.

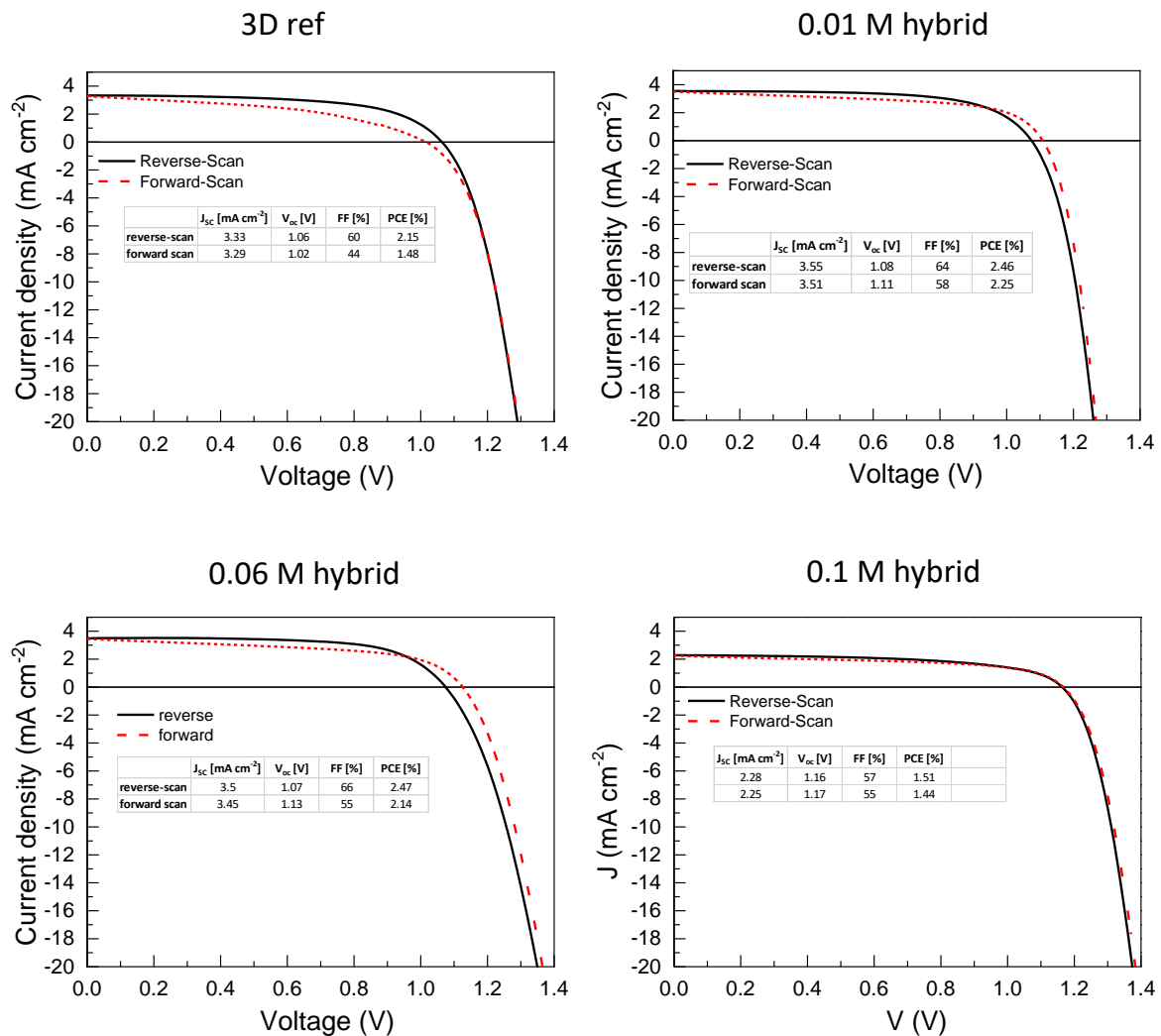


Figure S 4:  $J$ - $V$  curves of the solar cells investigated in this paper. The curves show rather low hysteresis between the forward and the reverse scan.

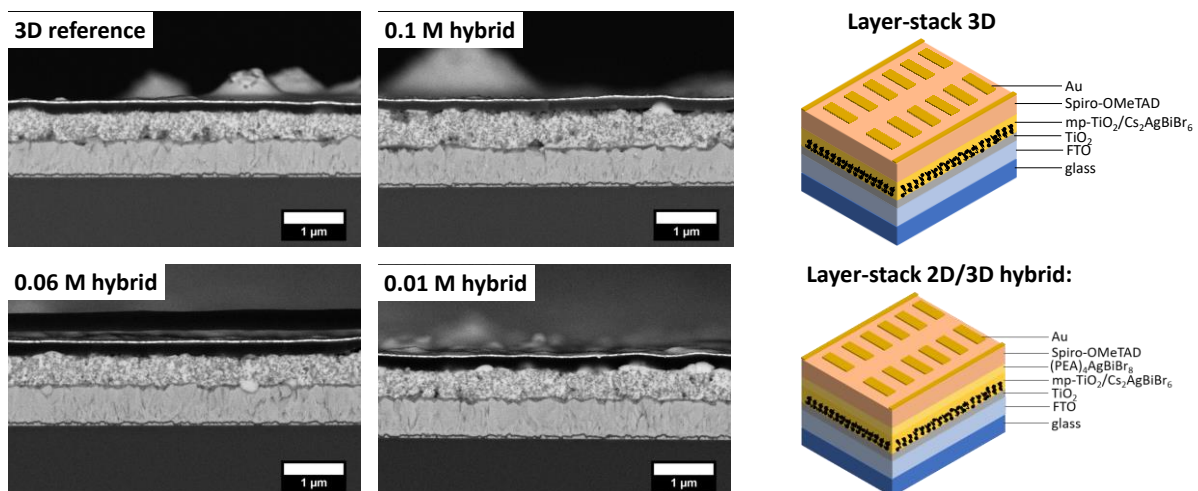


Figure S 5: SEM cross-sections of the investigated solar cells. On the right, the layer-stacks of the 3D perovskite and the 2D/3D hybrid perovskite solar cells are shown.

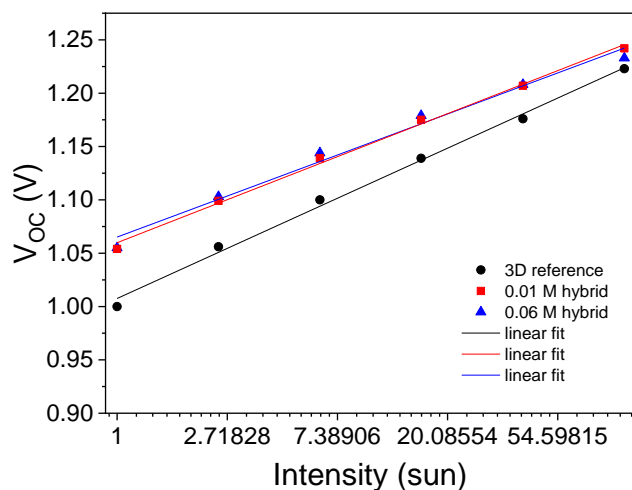


Figure S 6: Semi-ln plots of the light intensity dependent  $V_{OC}$  measurements. The parameters are shown as indicated in the legend.

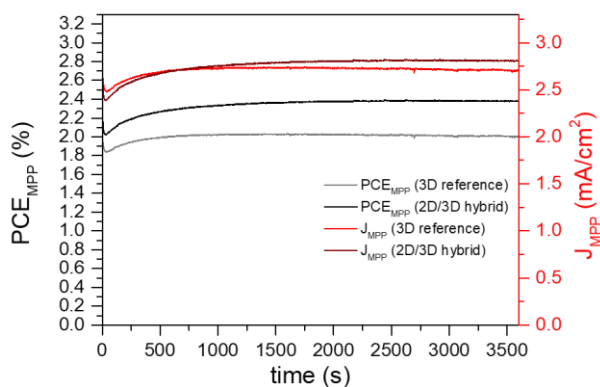
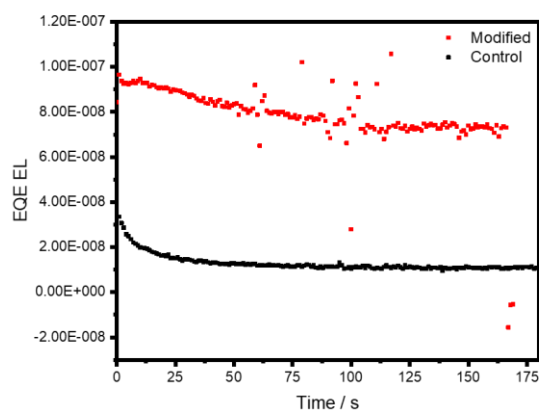


Figure S 7: EQE EL and MPP measurements of the 0.01 M (red line) and the 3D reference (black line) solar cells.

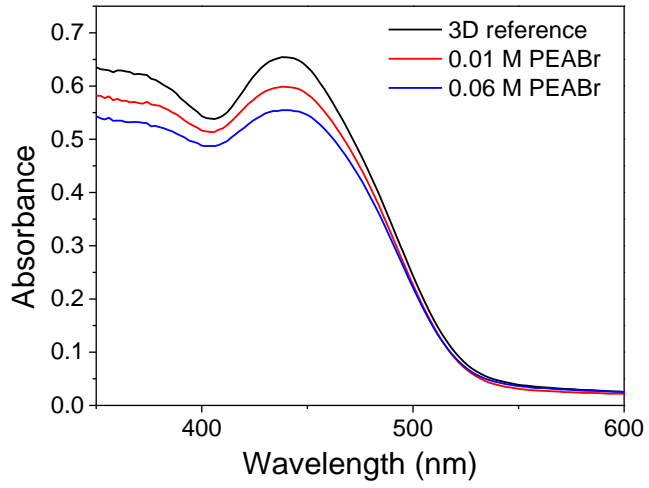


Figure S 8: UV-Vis absorption spectra obtained from thin films on FTO substrates. Color coding as indicated in the legend.



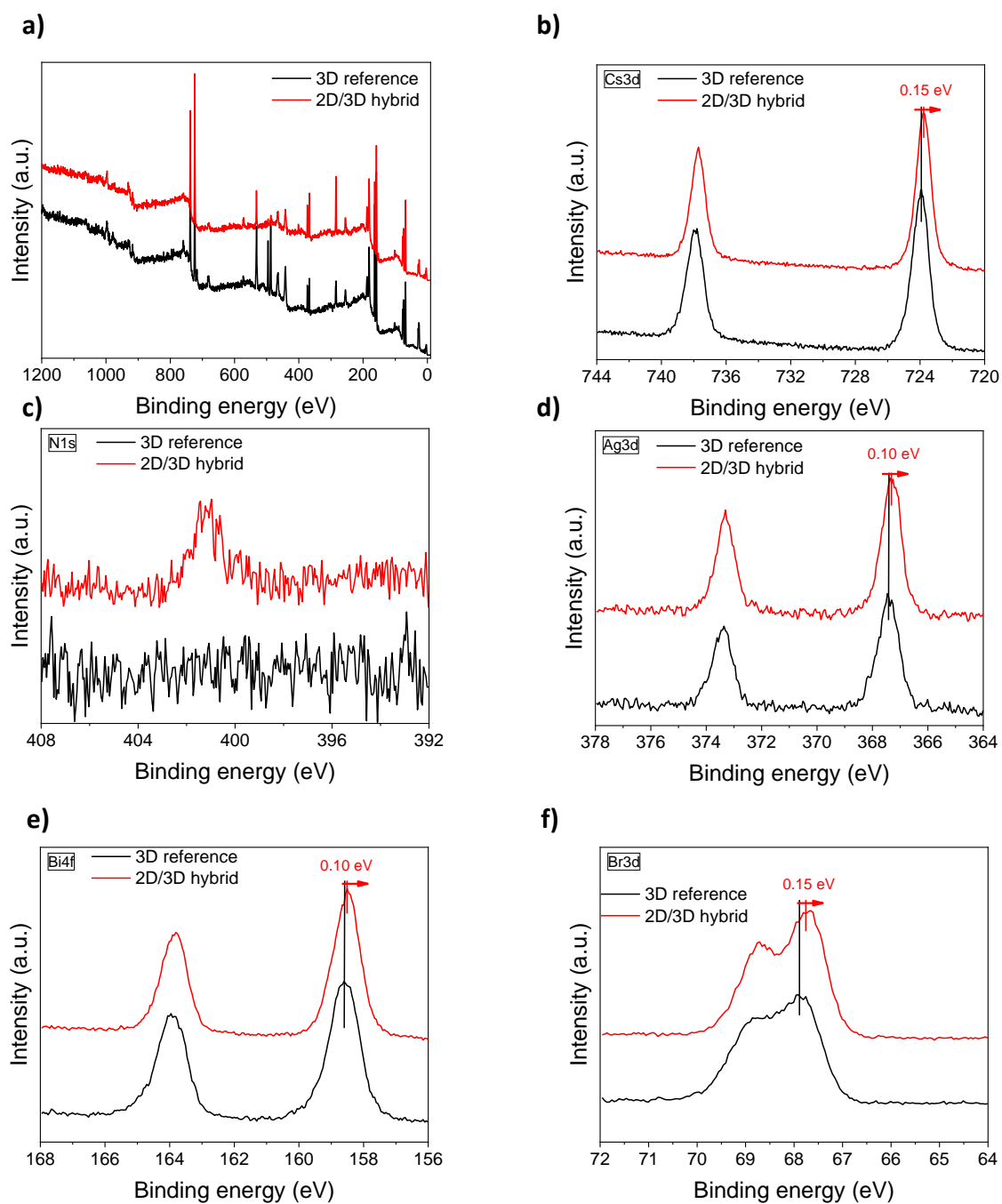


Figure S 9: XPS spectra of the 2D/3D hybrid (red lines) and 3D reference (black line) thin films. a) Survey, b) Cs3d, c) N1s, d) Ag3d, e) Bi4f and f) Br3d, all expressing shifts of 100 or 150 meV.

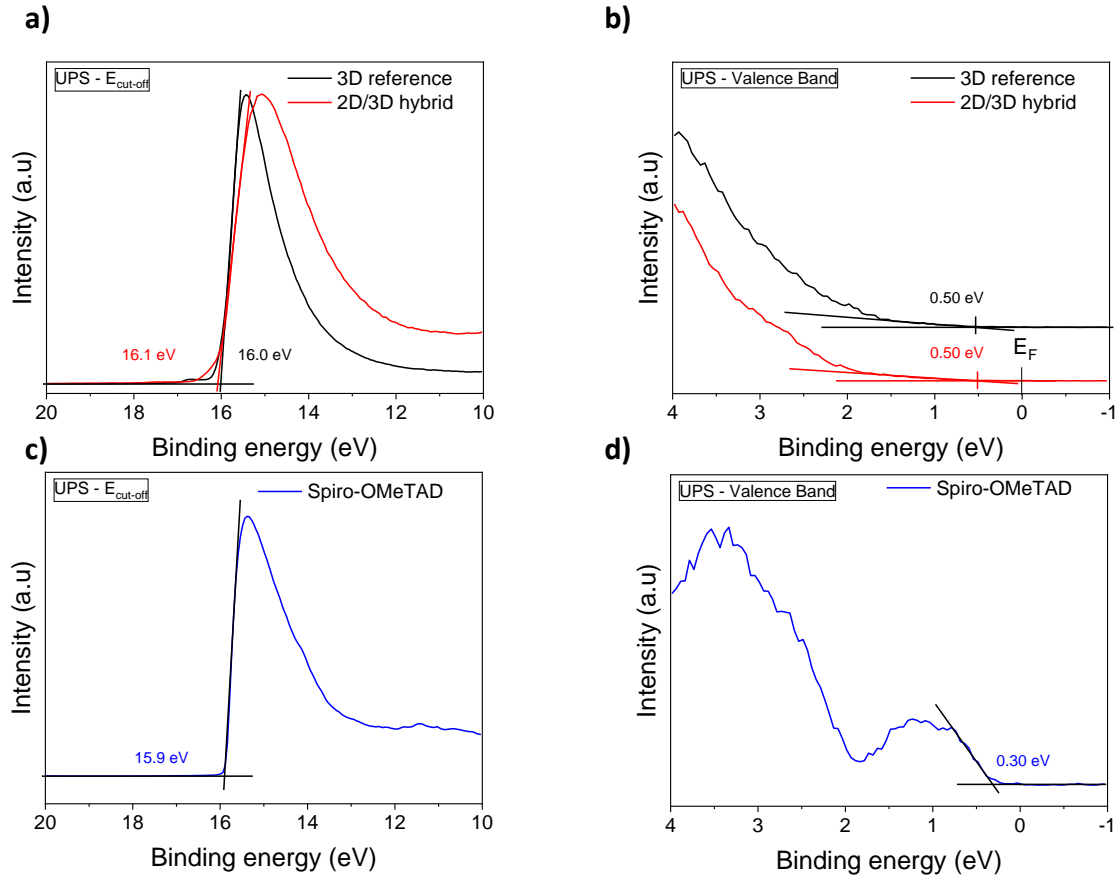


Figure S 10: UPS spectra of the 2D/3D hybrid (red lines) and 3D reference (black line) thin films. a) Cut-off measured by applying a 6V bias, b) valence band edge. UPS spectra of doped Spiro-OMeTAD with LiTFSI thin film. c) Cut-off measured by applying a 6V bias, d) valence band edge.

The Cut-off ( $E_{cut-off}$ ) provides the work function ( $W_f$ ) of the material (the distance between the vacuum level and the Fermi level) through this equation:  $W_f = h\nu - E_{cut-off}$ , with  $h\nu$  the excitation energy, i.e. the He I discharge (21.2 eV).

The doped Spiro-OMeTAD thin film was prepared inside the ultra-high vacuum system and directly transferred to the analytic chamber for UPS analysis. It was prepared by the co-evaporation of LiTFSI and Spiro-OMeTAD. The base pressure of the deposition chamber was  $6.0 \cdot 10^{-8}$  mbar and it increased to  $2.5 \cdot 10^{-7}$  mbar during the deposition process. A current of 625 mA and of 434 mA was applied to the  $Al_2O_3$  crucibles containing, respectively, Spiro-OMeTAD and LiTFSI. Co-evaporation lasted 2 hours.

The VBM of the 3D reference and the 2D/3D hybrid perovskite were measured similarly with UPS. We believe that the preparation or the transfer of the samples to Darmstadt might have induced some surface contaminations. The escape depth of the photoelectrons is higher for

XPS than for UPS. Therefore, XPS measurements are less influenced by these contaminations and are more reliable. However, it should be pointed out that the main conclusion of this section remains unchanged if we take the VBM difference obtained with XPS or with UPS. Because of the optical band gap difference a 0.15 eV (XPS) difference or a 0 eV (UPS) difference still induce an additional electron blocking layer at the 2D/3D interface.

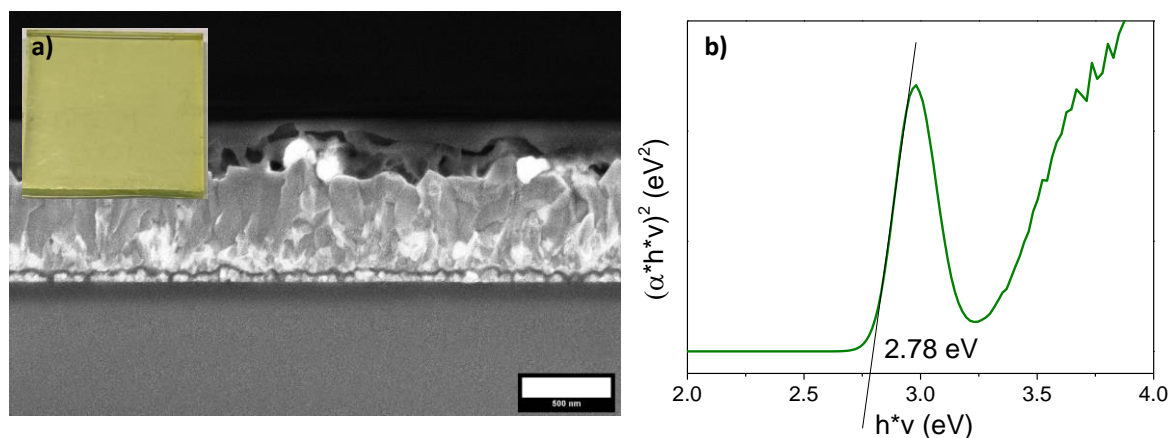


Figure S 11: a) SEM cross-sectional image of the measured  $(\text{PEA})_4\text{AgBiBr}_8$  thin films with a photograph in the inset. b) Direct Tauc plot of pure  $(\text{PEA})_4\text{AgBiBr}_8$  thin films on FTO.

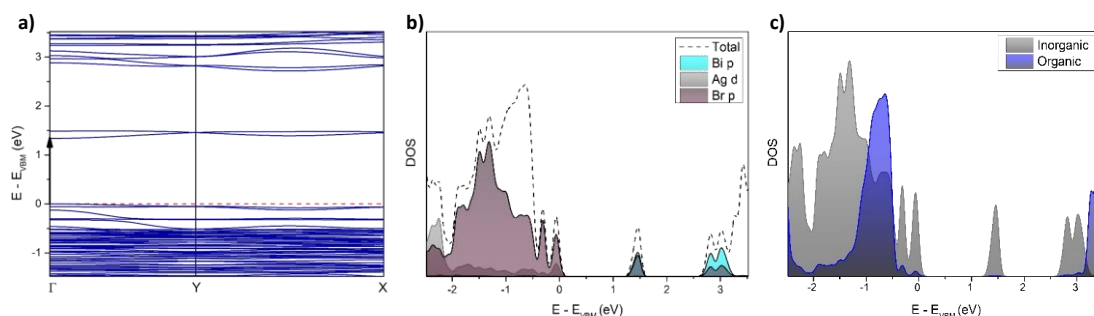


Figure S 12: Band structure calculations. a) Shows the PBE-SOC-TS band structure of  $(\text{PEA})_4\text{AgBiBr}_8$ , showcasing the characteristic conduction band splitting of the Bi 6p orbitals (b), already well described for  $\text{Cs}_2\text{AgBiBr}_6$ .<sup>[1]</sup> Furthermore, the band gap nature changes drastically, with the lowest band transition being centered at the  $\Gamma$  point in the Brillouin zone.<sup>[2]</sup> The absolute band gap is underestimated significantly ( $\sim 1.3$  eV), a known deficiency of the DFT-PBE method, whereas other characteristics like the electronic nature are expected to be predicted accurately.<sup>[3]</sup> The atomic contribution to the frontier orbitals is also identical to other previously published 2D Ag-Bi phases, consisting of mostly halide p and Ag d orbitals in the valence band, with the conduction band predominantly made up of Bi p and a contribution of halide p orbitals.<sup>[2,4]</sup>

## References

- [1] M. R. Filip, S. Hillman, A. A. Haghighirad, H. J. Snaith, F. Giustino, *J. Phys. Chem. Lett.* **2016**, 7, 2579.
- [2] B. A. Connor, L. Leppert, M. D. Smith, J. B. Neaton, H. I. Karunadasa, *J. Am. Chem. Soc.* **2018**, 140, 5235.
- [3] P. J. Hasnip, K. Refson, M. I. J. Probert, J. R. Yates, S. J. Clark, C. J. Pickard, *Philos. Trans. A Math. Phys. Eng. Sci.* **2014**, 372, 1.
- [4] M. K. Jana, S. M. Janke, D. J. Dirkes, S. Dovletgeldi, C. Liu, X. Qin, K. Gundogdu, W. You, V. Blum, D. B. Mitzi, *J. Am. Chem. Soc.* **2019**, 141, 7955.